DOI: 10.1002/ejoc.200600648

# Manganese Porphyrin Hosts as Epoxidation Catalysts – Activity and Stability Control by Axial Ligand Effects

**Johannes A. A. W. Elemans,*[a] Edward J. A. Bijsterveld,[a] Alan E. Rowan,*[a] and Roeland J. M. Nolte[a]**

**Keywords:** Manganese porphyrins / Supramolecular chemistry / Host–guest chemistry / Catalysis / Epoxidation

The catalytic performance of a cavity-containing [(porphyrin)Mn] in the epoxidation of alkenes is described. Inside the catalyst cavity, nitrogen-containing axial ligands can be bound to the porphyrin metal with high association constants, resulting in strong activation of the catalyst in the presence of only one equivalent of the ligand. Complexation of a sterically demanding ligand to the outside of the cavity-containing catalyst can prevent catalyst decomposition through the formation of μ-oxo dimers.



## Introduction

A wide variety of metalloporphyrins function as active sites in enzymes, such as in cytochrome P-450.[1] This monooxygenase oxidizes a range of alkanes and alkenes and is of fundamental importance for detoxification in the human body. The active site of the enzyme contains a $Fe^{III}$ protoporphyrin IX to which a cysteinate ligand essential for catalytic activity is axially coordinated.[2] During the past decade, a myriad of synthetic model systems that mimic the activity and selectivity of the natural enzyme have been developed,[3] although because of the only moderate stability of $Fe^{III}$-porphyrins in combination with cysteinate axial ligands, many of these model systems have been based on more stable and versatile $Mn^{III}$-porphyrins and N-containing axial ligands.[4] The use of molecular oxygen as an oxidant in model systems has appeared to be troublesome, because both the catalyst and the oxidant have to be activated by a reducing agent,[5] and so a variety of single-oxygen donor species – such as hypochlorites,[6] iodosylarenes,[7] peracids,[8] monopersulfates,[9] pyridine *N*-oxides,[10] alkyl hydroperoxides[11] and hydrogen peroxide – have been used as alternatives.[12]

In our[13] and other groups[14] the use of manganese porphyrins as oxidation catalysts in combination with hypochlorite as oxidant has been extensively studied. The presence of axial ligands such as pyridines or imidazoles appeared to enhance the reaction rates and the stereoselectivity of the reaction[15] by facilitating the formation and stabilization of the proposed formally $Mn^{V}$=O intermediate, preventing its dimerization into an unreactive and autodestructive μ-oxo $Mn^{IV}$-porphyrin dimer. A drawback for the optimal use of this system, however, is the need for a large excess (ca. 500 equiv.) of axial ligand because of its relatively weak binding to the porphyrin metal.

We have developed metal-porphyrins each appended with a diphenylglycoluril-based cavity, which effectively shields one side of the porphyrin plane.[16] The cavity is capable of binding N-containing axial ligands very strongly as the result of a combination of metal–ligand coordination and cavity-filling effects. Here the catalytic performance of the cavity-containing porphyrin catalyst **Mn1** in the epoxidation of alkenes is described in terms of activity, selectivity and stability, in the presence of several strongly binding axial ligands.[17]

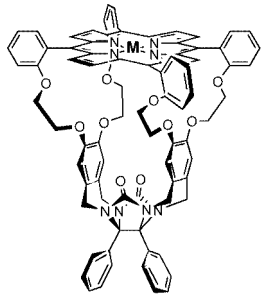

**$H_2$1** M = 2H
**Zn1** M = Zn
**Mn1** M = MnCl

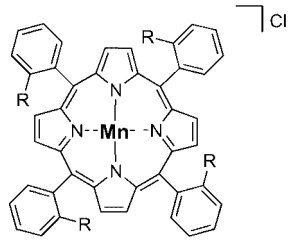

**MnTPP** R = H
**MnTMPP** R = OMe

## Results and Discussion

### Synthesis

The synthesis of **$H_2$1**, the free-base precursor of **Mn1**, has been described before,[16] but an alternative synthetic

[a] Institute for Molecules and Materials, Radboud University Nijmegen,
Toernooiveld, 6525 ED Nijmegen, The Netherlands
E-mail: J.Elemans@science.ru.nl
A.Rowan@science.ru.nl

   

route that has dramatically increased the yield of $\mathbf{H_21}$ (see Scheme 1) has been developed. Previously, $\mathbf{H_21}$ was synthesized in two steps from the tetratosylate derivative **2** by a quadruple alkylation of this compound with salicylic aldehyde and a subsequent condensation of the resulting tetraaldehyde with pyrrole to close the porphyin "roof".[16] The overall yield of these two reactions amounted to 3.8%. In the new procedure, host **2** was treated directly with one equivalent of the *meso*-tetrakis(2-hydroxyphenyl)porphyrin **3** under high-dilution conditions in acetonitrile in the presence of base to yield $\mathbf{H_21}$ in a yield of 30%. **Mn1** was synthesized from $\mathbf{H_21}$ by treatment with $Mn(OAc)_2{\cdot}4H_2O$ in DMF at reflux and subsequent ion exchange by stirring a solution of the product in chloroform with aqueous sodium chloride.

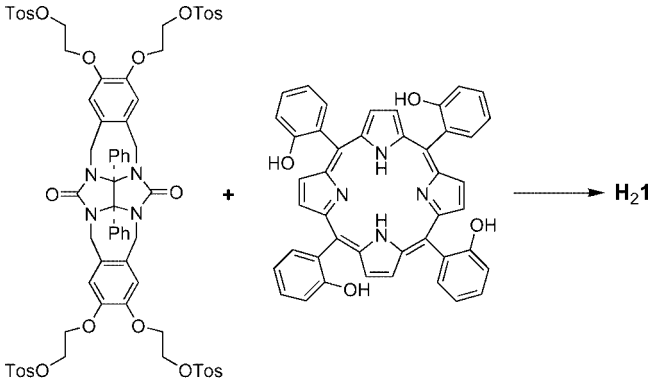


Scheme 1.

## Binding of Axial Ligands

The glycoluril-based cavity of **Mn1** has a diameter of approximately 9 Å and is capable of accommodating small axially binding ligands. Since their binding strength would be expected to have a great influence on the catalytic properties of **Mn1**, it was desired to determine the association constants ($K_a$ values) between these ligands and the host. However, since the determination of association constants of paramagnetic manganese porphyrins by NMR and UV/Vis spectroscopy is very difficult, cavity **Zn1**[16] was used as a reference material.[20] $^1$H NMR and UV/Vis titrations were carried out to establish the binding strength of **Zn1** with a number of pyridine and imidazole derivatives (Table 1), and pyridine (Py) was found to bind in the cavity of **Zn1** very strongly (Figure 1, a), an event accompanied by large upfield shifts in the crown ether proton signals of the host. In contrast with this very strong binding, the $K_a$ value between the bulky ligand 4-*tert*-butylpyridine (Bupy) and **Zn1** is low, which is attributed to Bupy being able to bind only to the outside of **Zn1** and hence not experiencing the stabilizing effects of the cavity (Figure 1, b). This was also evident from the absence of any shifts of the receptor side-wall and crown ether spacer proton signals in the NMR spectrum upon the addition of this ligand. Substitution of the pyridine ring with a *meta*-hydroxy group (OHPy) causes an enormous increase in binding strength relative to that of Py, because the ligand, as well as coordinating to the metal, simultaneously forms a strong hydrogen bond with one of the carbonyl groups of **Zn1**. 3-(Acetylamino)pyridine (AcAmPy) and 3-(4-toluoylamino)pyridine (TolAmPy) can also hydrogen bond to the carbonyl groups, but these hydrogen bonds are apparently weaker, since $K_a$ values similar to that between **Zn1** and Py are observed. Imidazole (Im) forms a stronger complex than Py with **Zn1**, which is not unexpected since the latter ligand is a weaker base. Molecular modelling studies revealed Im to be too small to coordinate to the zinc ion and at the same time form a hydrogen bond with one of the carbonyl groups of the host, but a

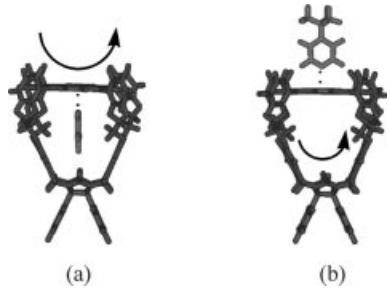


Figure 1. Approaches in which **Mn1** is used as an epoxidation catalyst in combination with Py (left, binding inside the cavity) or with BuPy (right, binding outside the cavity) as the axial ligands. The arrows indicate where the epoxidation reaction takes place.

Table 1. Association constants ($K_a$ [$M^{-1}$]) of complexes formed between **Zn1** and various axial ligands,[a] and epoxidation of olefins with **Mn1** and *one* equivalent of axial ligand.[b]

| Ligand[c] | $K_a$ | Epoxidation of α-pinene | | Epoxidation of *cis*-stilbene | | |
|---|---|---|---|---|---|---|
| | | $k_0$[d] | Yield[e] | $k_0$[d] | Yield[e] | *c:t*[f] |
| **Py** | $1.1{\cdot}10^5$ [g] | 12 | 81 | 20 [h] | 57 | 96:4 |
| **BuPy** | 625 [i] | 11 | 82 | 12 [h] | 57 | 90:10 |
| **OHPy** | $3.0{\cdot}10^7$ [j] | 34 | 44 | 21 [h] | 18 | –[k] |
| **AcAmPy** | $9.0{\cdot}10^4$ [g] | – | – | 15 [h] | 12 | – [k] |
| **TolAmPy** | $1.2{\cdot}10^5$ [g] | – | – | 28 [h] | 37 | 96:4 |
| **Im** | $3.2{\cdot}10^5$ [g] | 17 | 82 | –[k] | – [k] | – [k] |
| **MeIm** | $7.0{\cdot}10^4$ [g] | 8 | 38 | – [k] | –[k] | – [k] |

[a] In chloroform solution at 298 K. [b] Standard reaction conditions. [c] See text for abbreviations. [d] Initial rate·$10^5$ mol dm$^{-3}$ s$^{-1}$. [e] Yield (%) after 3 h. [f] Ratio *cis*/*trans* epoxide product after 3 h. [g] Estimated error 20%. [h] Rate of formation of the *cis* epoxide. [i] Estimated error 10%. [j] Estimated error 30%. [k] Not determined.

  

clear drop in binding strength was observed when *N*-methylimidazole (MeIm) was used instead of Im as the ligand.

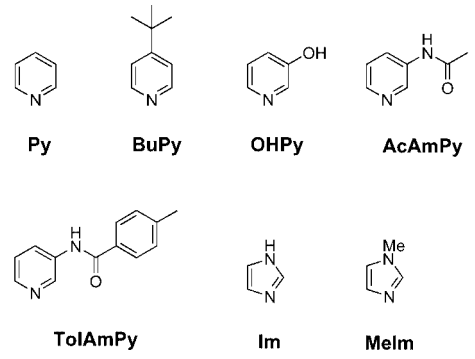


The $^1$H NMR spectra of the 1:1 host–guest complexes formed between **Zn1** and the two imidazole derivatives in $CDCl_3$ appeared to be strikingly different. In the spectra of the complex formed between **Zn1** and MeIm, all crown ether proton signals and the cavity side-wall proton signals of **Zn1** were shifted strongly upfield in relation to these signals in the free host, pointing to a host–guest geometry in which the aromatic surface of MeIm is oriented parallel to the cavity side-walls of **Zn1** (Figure 2, a), similarly to the geometries of the host–guest complexes formed between **Zn1** and the pyridine ligands. In contrast with this, the crown ether and side-wall proton signals in the complex formed between **Zn1** and Im were shifted only slightly upfield, indicating that the aromatic surface of Im is oriented perpendicular to the aromatic surface of the cavity side-walls (Figure 2, b). A 2D NOESY spectrum revealed that the ligand was still exclusively bound within the cavity and not to the outside of the porphyrin roof. It is not unlikely that the reason for the deviating binding geometry is the presence of an N–H···π interaction[21] between one of the cavity side-walls[22] and the Im NH proton.[23]

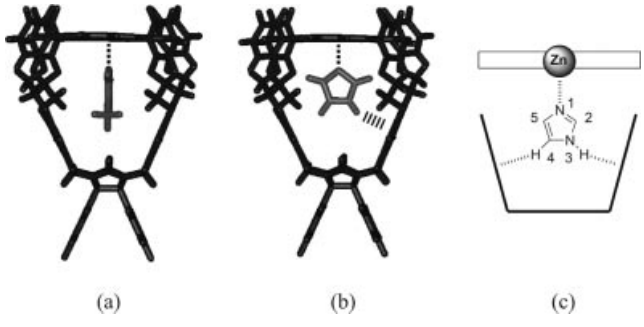


Figure 2. a) Computer-modelled host–guest geometry of the complex formed between **Zn1** and MeIm. b) Idem, of the host–guest complex formed between **Zn1** and **Im**, illustrating the possible N–H···π interaction between the guest and one of the side-walls of the host. c) Schematic picture of the coordination of Im to the zinc ion in the porphyrin roof of **Zn1** and possible simultaneous interaction between the Im 3-NH group and a cavity side-wall and the Im 4-CH group with the other cavity side-wall.

## Catalysis Studies

The strong binding of axial ligands in the cavity of **Zn1** is of great interest with regard to catalytic epoxidation reactions with **Mn1** as a catalyst, since as a result of the high binding constant it might be expected that only one equivalent of such a ligand might be needed to achieve ≥99% binding to the porphyrin metal. To investigate this assumption, the epoxidation of α-pinene was carried out with host **Mn1** as the catalyst and porphyrin **MnTPP** as the reference, in the presence of *one* equivalent of Py (Figure 1, a). **Mn1** appeared to display an initial rate ten times higher than that of **MnTPP** (Figure 3, Table 2), as a result of which it requires more than 10 h for the reaction to be complete in the case of **MnTPP**, but only 2 h in that of **Mn1**. The initial epoxidation rate is generally related to the binding constant of the axial ligand [i.e., the rate increases when the $K_a$ value of the ligand (measured with the related host **Zn1**) becomes higher (Table 1)].[24] It is notable that the most strongly binding ligand OHPy gives very high initial rates, but also the lowest yield after 3 h; the reason for this is probably the gradual expulsion of the ligand out of the cavity of **Mn1** as a result of deprotonation by the strongly basic $OCl^-$ species.[25] Such deprotonation was also observed for AcAmPy and to a lesser extent for TolAmPy. Surprisingly, deprotonation did not occur when Im was used, and in the case of this ligand the epoxidation reaction was complete within 1 h, giving an 82% yield of epoxide. In addition to a high epoxidation rate, a further advantage of the strong binding of Im is that its degradation (by oxidation), which in other systems has already been observed to occur at relatively low concentrations of the ligand,[26] is minimal. Apparently, its binding in the cavity of **Mn1** protects it from this undesired reaction.

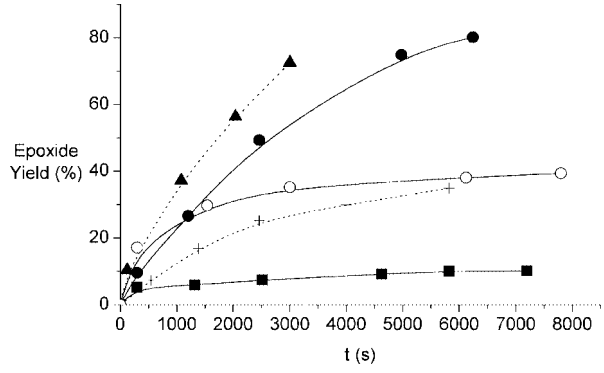


Figure 3. Product formation curves for the epoxidation of α-pinene, in the presence of *one* equivalent of an axial ligand. **Mn1-Im** (▲), **Mn1-Py** (●), **Mn1-OHPy** (o), **Mn1-MeIm** (+), **MnTPP-Py** (■).

In order to provide better understanding of the catalytic performance of **Mn1** in terms of activity and stereoselectivity, additional epoxidation experiments with manganese porphyrin catalysts and one equivalent of pyridine were carried out (Table 2). It is clear that the reference compound **MnTPP** is a very poor catalyst under these conditions. To rule out any electronic effects, **MnTMPP** was taken as a

  

Table 2. Epoxidation of olefins by **Mn1** and the reference catalysts **MnTPP** and **MnTMPP** in the presence of *one* equivalent of **Py** as the axial ligand.[a]

| Substrate | **Mn1** | | | **MnTPP** | | | **MnTMPP** | | |
|---|---|---|---|---|---|---|---|---|---|
| | $k_0$[b] | Yield[c] | *c*:*t*[d] | $k_0$[b] | Yield[c] | *c*:*t*[d] | $k_0$[b] | Yield[c] | *c*:*t*[d] |
| α-Pinene | 12 | 81 | | 1 | 10 | | – [e] | – [e] | – [e] |
| *cis*-Stilbene | 20[f] | 57 | 96:4 | 4[f] | 39 | 65:35 | 3[f] | 33 | 63:37 |
| *trans*-Stilbene | 19 | 72 | – [g] | 4 | 9 | – [g] | < 1 | 8 | – [g] |

[a] Standard reaction conditions. [b] Initial rate·$10^5$ mol dm$^{-3}$ s$^{-1}$. [c] Yield (%) after 3 h. [d] Ratio *cis*-*trans* epoxide product after 3 h. [e] Not determined. [f] Rate of formation of the *cis* epoxide. [g] No *cis* epoxide was detected.

second reference, but this catalyst showed even lower rates of epoxidation than **MnTPP**. These results demonstrate that the enhanced rate of epoxidation is produced primarily by the strong binding of pyridine inside the cavity of **Mn1** and not just by electronic effects of the porphyrin. In the case of the latter catalyst it can also be seen that the epoxidation is considerably more stereoselective for the conversion of *cis*-stilbene into *cis*-stilbene oxide, an effect that can be interpreted in terms of the strong coordination of the axial ligand, which pulls the metal centre into the plane of the porphyrin and thereby hinders the rotation of the C–C bond of the *cis*-stilbene substrate coordinated to the other face of the porphyrin in the transition state (Figure 4).[15]

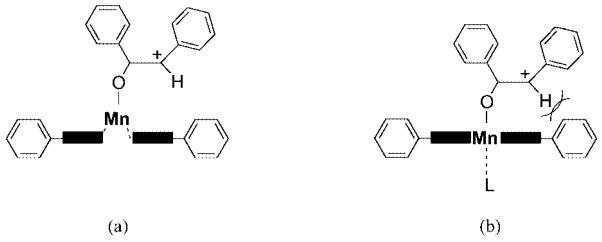


Figure 4. Proposed effect of an axial ligand **L** on the stereospecificity in the epoxidation of *cis*-stilbene a) in the absence of an axial ligand, and b) in the presence of an axial ligand, which pulls the metal center into the plane of the porphyrin, thereby sterically hindering the rotation of the C–C bond of the substrate coordinated to the other face of the porphyrin in the transition state.[15]

A major drawback of **MnTPP** and **MnTMPP** appeared to be their decomposition, attributed to the formation of $[(P)Mn^{IV}–O–Mn^{IV}(P)]^{2+}$ μ-oxo dimers, during the catalytic reaction. These dimers are unreactive in further catalysis and decompose through electrophilic attack on the electron-rich *meso* positions in the porphyrin ring.[13c] When a reactive substrate is present, it generally competes successfully with a $[(P)Mn^{III}X]^+$ molecule for the reactive $Mn^V$-oxo species, but the catalyst then rapidly decomposes once all the substrate is converted, as is visible in the bleaching of the brown reaction mixture. This decomposition also occurred in the case of the systems of **Mn1** with one equivalent of a strongly binding axial ligand present.

To prevent this decomposition the bulky axial ligand Bupy was used in combination with **Mn1**, as it was reasoned that coordination of this ligand (which does not fit within the cavity of the catalyst) would efficiently prevent μ-oxo dimer formation, including after all of the substrate had been converted, since the other face of the porphyrin is protected by the receptor cavity (Figure 1, b). Indeed, when epoxidation experiments with **Mn1** were carried out in the presence of 500 equiv. of Bupy (Table 3), catalyst destruction did not occur, as was already indicated by the fact that the organic layer retained its brown colour even after the reaction mixture had been stirred in the absence of substrate for more than a week. More importantly, however, was the observation that freshly added portions of substrate were epoxidized with similar initial rates as the first portion without any apparent deterioration of the catalyst, thus affording high turnover numbers per **Mn1** molecule (>1000).[27] Under the same conditions, **MnTPP** and **MnTMPP** were not stabilized by Bupy and decomposed rapidly.

Whereas the initial conversion rates for the epoxidation of α-pinene and *trans*-stilbene do not significantly differ for the three catalysts, there is a clear drop in rate for the epoxidation of *cis*-stilbene, going from **MnTPP** > **MnTMPP** > **Mn1**. This decrease coincides with an increase in steric hindrance imposed by the substituents of the *meso*-phenyl rings of the catalysts, which apparently only affects the conversion of *cis*- and not of *trans*-stilbene. The very low rate observed when **Mn1** is the catalyst can be explained by the fact that the rather bulky *cis*-stilbene would be expected to experience severe hindrance by the confinement of the host

Table 3. Epoxidation of olefins by **Mn1** and the reference catalysts **MnTPP** and **MnTMPP** in the presence of 500 equiv. of **BuPy** as the axial ligand.[a]

| Substrate | **Mn1** | | | **MnTPP** | | | **MnTMPP** | | |
|---|---|---|---|---|---|---|---|---|---|
| | $k_0$[b] | Yield[c] | *c*:*t*[d] | $k_0$[b] | Yield[c] | *c*:*t*[d] | $k_0$[b] | Yield[c] | *c*:*t*[d] |
| α-Pinene | 11 | 82 | | 13 | 80 | | – [e] | – [e] | – [e] |
| *cis*-Stilbene | 12[f] | 57 | 90:10 | 57[f] | 70 | 90:10 | 39[f] | 52 | 92:8 |
| *trans*-Stilbene | 24 | 72 | – [g] | 21 | 63 | – [g] | 20 | 65 | – [g] |

[a] Standard reaction conditions. [b] Initial rate·$10^5$ mol dm$^{-3}$ s$^{-1}$. [c] Yield (%) after 3 h. [d] Ratio *cis*-*trans* epoxide product after 3 h. [e] Not determined. [f] Rate of formation of the *cis* epoxide. [g] No *cis* epoxide was detected.

  

cavity, which it has to enter completely to reach the reactive manganese oxo species, whereas molecular modelling studies show this steric hindrance for the much flatter *trans* isomer to be negligible (Figure 5).

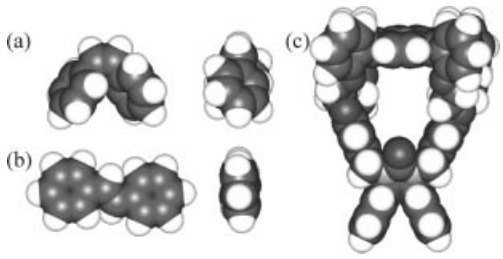


Figure 5. a) Computer-modelled space-filling structure of *cis*-stilbene (side view and view along the double bond). b) Idem, of *trans*-stilbene. c) Computer-modelled space-filling structure of **Mn1** showing the size of the cavity. All compounds are displayed on the same scale.

## Conclusions

We have shown that very strong binding of axial ligands can be achieved through their complexation to a manganese porphyrin functionalized with a substrate binding cavity based on diphenylglycoluril. As a result of this strong binding, only one equivalent of ligand is required to achieve a >99+% occupation of the manganese metal, which is reflected in a high activity in the catalytic epoxidation of olefins by this system. In a different approach, a bulky axial ligand was complexed exclusively to the outside of the cavity, which effectively protected the catalyst from μ-oxo dimer formation and thus assured its stability over several rounds of catalysis. Currently, the latter system is being employed by our group as a very stable processive catalyst in the epoxidation of polyolefin substrates.[28]

## Experimental Section

**General:** All solvents were distilled under nitrogen prior to use. Acetonitrile was distilled from $CaH_2$, chloroform from $CaCl_2$, dichloromethane from $CaH_2$, and DMF from BaO. $K_2CO_3$ was dried in an oven (150 °C). Pyrrole was distilled at room temperature under reduced pressure prior to use. All other solvents and chemicals were commercial materials and were used without further purification. Merck silica gel (60 H) was used for column chromatography and Merck silica gel plates (F254) for thin layer chromatography. $^1$H NMR and $^{13}$C NMR spectra were recorded on Bruker DPX 200, Bruker DMX 300 and Bruker DRX 500 instruments. Chemical shifts are reported in ppm downfield from internal TMS ($\delta$ = 0.00 ppm) in the case of $^1$H NMR spectra in $CDCl_3$. In the case of $^{13}$C NMR spectra, the solvent peak was used as a reference ($CDCl_3$: δ = 77.0 ppm). Symbols used are: s = singlet, d = doublet, dd = doublet of doublets, m = multiplet, br = broad. EI and FAB mass spectra were recorded on a VG 7070E and a Finnigan MAT 900 S instrument. The matrix used for FAB was *m*-nitrobenzyl alcohol. Elemental analyses were determined with a Carbo Erba Ea 1108 instrument. UV/Vis spectra were measured on a Varian Cary 50 UV/Vis spectrophotometer. GC spectra were measured on a Varian GC3800 instrument with a 8200 CX autosampler. Melting points were recorded on a Jeneval THMS 600 hot-stage polarization microscope and are uncorrected. Molecular modelling calculations were performed on a Silicon Graphics Indigo II work station with use of the CHARMm force field.[18]

**Syntheses**

***meso*-Tetrakis(2-hydroxyphenyl)porphyrin ($H_2$THPP):** *meso*-Tetrakis(2-methoxyphenyl)porphyrin[19] (1.15 g, 1.6 mmol) was dissolved in $CH_2Cl_2$ (20 mL), the solution was cooled to –25 °C, and $BBr_3$ (3 mL) was added. This mixture was slowly warmed to room temperature, stirred overnight under a nitrogen atmosphere and subsequently poured into ice/water (150 mL), to which ethyl acetate (350 mL) was added. $NaHCO_3$ was added carefully until the organic layer became purple, the organic phase was washed with saturated aqueous $NaHCO_3$ and dried with $MgSO_4$, and the solvents were evaporated to dryness. The product was purified by column chromatography [silica, 5% MeOH in $CHCl_3$ (v/v)] to yield **$H_2$THPP** (0.98 g, 92%) as a purple solid. $^1$H NMR ($CDCl_3$, 300 MHz): $\delta$ = 8.91 (s, 8 H, β-pyrrole), 8.02–7.91 (m, 4 H, ArH), 7.79–7.67 (m, 4 H, ArH), 7.42–7.28 (m, 8 H, ArH), 6.9–6.8 (br. s, 4 H, OH), –2.73 (br. s, 2 H, NH) ppm. FAB-MS: *m*/*z* = 679 [M + H]$^+$.

**Porphyrin Host $H_2$1:** A solution of host 2 (750 mg, 0.55 mmol), porphyrin **3** (375 mg, 0.55 mmol) and $K_2CO_3$ (750 mg, 5.4 mmol) in degassed acetonitrile (700 mL) was heated at reflux under nitrogen for 16 h. After cooling, the mixture was filtered, the filtrate was evaporated to dryness, and the product was purified by column chromatography (alumina Act. III, $CHCl_3$) to yield **$H_2$1** (220 mg, 30%) as a purple powder. Physical properties were in agreement with those previously reported.[16]

**Porphyrin Host Mn1:** A degassed solution of **$H_2$1** (25 mg, 19 μmol) in DMF (2 mL) was heated to reflux. $Mn(OAc)_2{\cdot}4H_2O$ (10 mg, 41 μmol) was added and the mixture was heated at reflux under nitrogen for 2 h. After cooling, the solvent was evaporated to dryness and the residue was dissolved in $CHCl_3$ (10 mL). A saturated aqueous NaCl solution (10 mL) was added, the mixture was stirred vigorously for 16 h, the organic layer was extracted with water (3 × 50 mL), and the solvents were evaporated to dryness. The residue was purified by column chromatography (silica, $CHCl_3$/MeOH 9:1, v/v, $R_f$ = 0.17), the product was dissolved in a minimal amount of $CHCl_3$, and this solution was added dropwise to stirred *n*-hexane. After centrifugation, the product was dried under vacuum to yield **Mn1** (26 mg, 97%) as dark green needles. M.p. > 400 °C. IR (KBr pellet): $\tilde{\nu}$ = 3048 (ArH), 2923, 2854 ($CH_2$), 1696 (C=O), 1600, 1580, 1513, 1462, 1449, 1427 (C=C), 1308, 1279, 1249, 1204 ($CH_2$), 1107, 1064, 1010 (COC) cm$^{-1}$. UV/Vis ($CH_2Cl_2$): $\lambda$/nm [log($\varepsilon$/M$^{-1}$cm$^{-1}$)] = 346 (4.55), 375 (4.66), 409 (4.54), 450 (3.70), 480 (4.96), 527 (3.40), 586 (3.54), 617 (3.50). FAB-MS: *m*/*z* = 1397 [M – Cl]$^+$. $C_{84}H_{62}N_8O_{10}MnCl$ (1433.85): calcd. C 70.44, H 4.29, N 7.82; found: C 70.12, H 4.14, N, 8.12.

**3-Acetyliminopyridine (AcAmPy):** 3-Aminopyridine (1.00 g, 10.6 mmol) was dissolved in acetone (150 mL), and $K_2CO_3$ (7.4 g, 54 mmol) was added, followed by the dropwise addition of acetyl chloride (2.5 g, 32 mmol) in acetone (5 mL). The reaction mixture was stirred for 3 h, after which it was quenched by the addition of water and the solvent was removed by evaporation. The residue was taken up in $CH_2Cl_2$ and this solution was washed with water, while the organic layer was dried with $Na_2SO_4$, and after filtration was evaporated to dryness. The product was purified by column chromatography (silica, 5% MeOH in $CHCl_3$), and then recrystallized from toluene. Yield: 1.18 g (82%). M.p. 131.5 °C. $^1$H NMR ($CDCl_3$, 300 MHz): $\delta$ = 8.55 (s, 1 H, PyH-2), 8.35 (d, $^3J$ = 4.1 Hz, 1 H, PyH-6), 8.18 (d, $^3J$ = 8.2 Hz, 1 H, PyH-4), 7.80 (br s, 1 H,

  

NH), 7.40–7.20 (m, 1 H, PyH-3), 2.22 (s, 3 H, $CH_3$) ppm; $^{13}C\{^1H\}$NMR ($CDCl_3$, 75 MHz): $\delta$ = 169.25, 144.83, 140.93, 135.25, 127.44, 123.82, 24.17 ppm. EI-MS: $m/z$ = 136 $[M]^+$. $C_7H_8N_2O$ (136.15): calcd. C 61.75, H 5.92, N 20.58; found: C 62.10, H 5.91, N 19.81.

**3-(4-Toluoylamino)pyridine (TolAmPy):** 3-Aminopyridine (5.00 g, 53.1 mmol) was dissolved in pyridine (60 mL), *p*-toluoyl chloride (15 mL, 113 mmol) was added slowly to this solution, and the mixture was stirred overnight at room temperature. Aqueous HCl (1 N, 100 mL) and ethyl acetate (100 mL) were added. After phase separation, the aqueous phase was neutralized with aqueous NaOH (1 N), the mixture was filtered, and the residue was recrystallized from water, affording **TolAmPy**. Yield: 3.86 g (34%). M.p. 126.5 °C. $^1H$ NMR ([D$_6$]DMSO, 200 MHz): $\delta$ = 10.45 (br s, 1 H, NH), 8.98 (s, 1 H, PyH-2), 8.34 (d, $^3J$ = 4.1 Hz, 1 H, PyH-6), 8.24 (d, $^3J$ = 8.5 Hz, 1 H, PyH-4), 7.95 (d, $^3J$ = 8.1 Hz, 2 H, ArH), 7.5–7.3 (m, 3 H, PyH-5 and ArH), 2.43 (s, 3 H, $ArCH_3$) ppm; $^{13}C\{^1H\}$NMR ($CDCl_3$, 75 MHz): $\delta$ = 165.96, 145.40, 142.96, 141.39, 131.30, 129.58, 127.51, 127.08, 123.78, 21.53 ppm. EI-MS: $m/z$ = 212 $(M^+)$. $C_{13}H_{12}N_2O\cdot0.4H_2O$ (219.46): C 71.15, H 5.88, N 12.77; found: C 71.57, H 5.46, N 12.30.

**MnTMPP:** Compound **$H_2$TMP** (100 mg, 0.136 mmol) was dissolved in DMF (10 mL) and the system was heated to reflux. $Mn(OAc)_2\cdot4H_2O$ (168 mg, 0.686 mmol) was added and the reaction was monitored by UV/Vis spectroscopy. After 30 min, the reaction was complete and the solvent was evaporated. $CH_2Cl_2$ (10 mL) and saturated aqueous NaCl solution (10 mL) were added and the resulting mixture was stirred at room temperature overnight. The organic layer was separated, dried with $MgSO_4$, evaporated to dryness and subjected to column chromatography (silica, 2–10% MeOH in $CHCl_3$). The product was dissolved in the smallest possible amount of $CHCl_3$ and precipitated from *n*-hexane. Yield: 103 mg (92%) of **MnTMPP** as a dark green solid. UV/Vis ($CH_2Cl_2$): $\lambda$/nm [log($\varepsilon$/M$^{-1}$ cm$^{-1}$)] = 348 (4.60), 374 (4.69), 400 (4.58), 449 (4.07), 479 (5.01), 527 (3.74), 582 (3.97), 618 (3.92). FAB-MS: $m/z$ = 787 $[M - Cl]^+$.

**Catalysis Experiments:** Catalysis experiments were carried out in a Schlenk tube (2 × 2 × 12 cm) under nitrogen. Substrate (0.6 M), phase-transfer catalyst (tetra-*n*-butylammonium chloride, 5.0 mM), the axial ligand (approach A: 2.5 mM; approach B: 1.25 M) and the internal standard (1,3,5-tri-*tert*-butylbenzene, 0.6 mM) were added to a solution of distilled $CH_2Cl_2$ containing Mn-porphyrin (2.5 mM, 650 μL), together with an aqueous solution of NaOCl (0.6 M , 2.0 mL). The resulting two-phase system was magnetically stirred at 1100 rpm. At intervals, the stirrer and timer were stopped, and after phase separation an aliquot (1 μL) was withdrawn from the organic phase and injected into $CH_2Cl_2$ (0.5 mL). The resulting $CH_2Cl_2$ solution was analysed by GC and compared with authentic samples. After 3 h, the organic phase was evaporated to dryness and analysed by $^1H$ NMR spectroscopy.

## Acknowledgments

The Dutch National Research School for Combination Catalysis (NRSC-C) and the Council for the Chemical Sciences of the Netherlands Organization for Scientific Research (CW-NWO) are acknowledged for financial support to J. A. A. W. E. (Veni grant), A. E. R. (Vidi grant) and R. J. M. N. (Top grant).

[1] P. R. Ortiz de Montellano (Ed.), *Cytochrome P450: Structure, Mechanism and Biochemistry*, 2nd ed., Plenum Press, New York, **1995**.
[2] B. Meunier, S. P. de Visser, S. Shaik, *Chem. Rev.* **2004**, *104*, 3947.
[3] a) M. C. Feiters, A. E. Rowan, R. J. M. Nolte, *Chem. Soc. Rev.* **2000**, *29*, 375; b) H. C. Zhou, J. T. Groves, *J. Porphyrins Phthalocyanines* **2004**, *8*, 125; c) W. D. Woggon, *Acc. Chem. Res.* **2005**, *38*, 127; d) S. Kozuch, T. Leifels, D. Meyer, L. Sbaragli, S. Shaik, W. D. Woggon, *Synlett* **2005**, 674; e) E. Rose, B. Andrioletti, S. Zrig, M. Quelquejeu-Ethève, *Chem. Soc. Rev.* **2005**, *34*, 573.
[4] B. Meunier, *Chem. Rev.* **1992**, *92*, 1411.
[5] I. Tabushi, *Coord. Chem. Rev.* **1988**, *86*, 1.
[6] a) J. P. Collman, J. L. Brauman, B. Meunier, T. Hayashi, T. Kodadek, *J. Am. Chem. Soc.* **1985**, *107*, 2000; b) F. Montanari, M. Penso, S. Quici, P. Vigano, *J. Org. Chem.* **1985**, *50*, 4888.
[7] a) J. T. Groves, W. J. Kruper, R. C. Haushalter, *J. Am. Chem. Soc.* **1980**, *102*, 6375; b) C. L. Hill, B. C. Schardt, *J. Am. Chem. Soc.* **1980**, *102*, 6374; c) A. J. Castellino, T. C. Bruice, *J. Am. Chem. Soc.* **1988**, *110*, 158; d) J. P. Collman, X. Zhang, R. T. Hembre, J. I. Brauman, *J. Am. Chem. Soc.* **1990**, *112*, 5356; e) E. Baciocchi, T. Boschi, L. Cassioli, C. Galli, L. Jaquinod, A. Lapi, R. Paolesse, K. M. Smith, P. Tagliatesta, *Eur. J. Org. Chem.* **1999**, 3281.
[8] L. C. Yuan, T. C. Bruice, *J. Am. Chem. Soc.* **1986**, *108*, 1643.
[9] a) B. de Poorter, B. Meunier, *J. Chem. Soc., Perkin Trans. 2* **1985**, 1735; b) A. Cagnina, S. Campestrini, F. di Furia, P. Ghiotto, *J. Mol. Catal. A* **1998**, *130*, 221.
[10] W. H. Wong, D. Osovic, T. C. Bruice, *J. Am. Chem. Soc.* **1987**, *109*, 3428.
[11] D. Mansuy, P. Battioni, J. P. Renaud, *J. Chem. Soc., Chem. Commun.* **1984**, 1255.
[12] P. Battioni, J. P. Renaud, J. F. Bartoli, M. Reina-Artiles, M. Fort, D. Mansuy, *J. Am. Chem. Soc.* **1988**, *110*, 8462.
[13] a) J. A. S. J. Razenberg, R. J. M. Nolte, W. Drenth, *Recl. Trav. Chim. Pays-Bas* **1986**, *105*, 103; b) R. J. M. Nolte, J. A. S. J. Razenberg, R. J. W. Schuurman, *J. Am. Chem. Soc.* **1986**, *108*, 2751; c) A. W. van der Made, R. J. M. Nolte, W. Drenth, *Recl. Trav. Chim. Pays-Bas* **1990**, *109*, 537.
[14] B. Meunier, E. Guilmet, M.-E. de Carvalho, R. Poilblanc, *J. Am. Chem. Soc.* **1984**, *106*, 6668.
[15] A. W. van der Made, R. J. M. Nolte, *J. Mol. Catal.* **1984**, *26*, 333.
[16] J. A. A. W. Elemans, M. B. Claase, P. P. M. Aarts, A. E. Rowan, A. P. H. J. Schenning, R. J. M. Nolte, *J. Org. Chem.* **1999**, *64*, 7009.
[17] A preliminary communication of this work has appeared: J. A. A. W. Elemans, E. J. A. Bijsterveld, A. E. Rowan, R. J. M. Nolte, *Chem. Commun.* **2000**, 2443.
[18] CHARMm Version 22.0, Revision 92.0911. Resident and Fellows of Harvard College, 1984, 1992, with the use of template charges.
[19] M. Monteneau, J. Mispelter, B. Loock, E. Bisagni, *J. Chem. Soc., Perkin Trans. 1* **1983**, 189.
[20] In UV/Vis titrations of **Mn1** with pyridine- and imidazole-containing ligands the Soret band at 480 nm displayed only a minimal increase in intensity after the addition of >10 equiv. of ligand, but no shift in wavelength. The obtained titration curves could not be fitted to give reliable association constants and for this reason host **Zn1** was used as a reference. Generally, the $K_a$ values of *N*-ligands with manganese porphyrins are somewhat lower than with zinc porphyrins.
[21] a) H. Adams, F. J. Carver, C. A. Hunter, N. J. Osborne, *Chem. Commun.* **1996**, 2529; b) T. Nakanaga, F. Ito, *J. Phys. Chem. A* **1999**, *103*, 5440.
[22] In addition to an NH···π interaction, there is also a possible CH···π interaction between the imidazole 4-proton and the other side-wall of the host; see part c of Figure 2.
[23] Unfortunately the Im proton signals in the spectrum of the complex were very broad, which prohibited their use as a diagnostic tool for the determination of the binding geometry of the ligand.

  

[24] It must be noted that the catalytic reactions were performed in a two-phase solvent mixture of dichloromethane in water, which would probably lower the $K_a$ values somewhat.
[25] The presence of the conjugated base of OHPy in the aqueous layer supported this conclusion.
[26] S. Campestrini, F. di Furia, P. Ghiotto, F. Novello, C. Travaglini, *J. Mol. Catal. A J. Mol. Catal.* **1996**, *105*, 17.
[27] Five portions of substrate were oxidized without any apparent decomposition of the catalyst. After that it became difficult to measure a reliable rate of conversion due to phase separation between the solvent and the epoxidation products.
[28] P. Thordarson, E. J. A. Bijsterveld, A. E. Rowan, R. J. M. Nolte, *Nature* **2003**, *424*, 915.

Received: July 26, 2006
Published Online: December 5, 2006

  